



ELSEVIER

Contents lists available at ScienceDirect

Continental Shelf Research

journal homepage: www.elsevier.com/locate/csr

Research papers

Variable temperature, salinity and water mass structures in the southwestern Taiwan Strait in summer

Jianyu Hu^{a,*}, Huasheng Hong^a, Yan Li^a, Yuwu Jiang^a, Zhaozhang Chen^a, Jia Zhu^a, Zhenwen Wan^a, Zhenyu Sun^a, Hongxing Liang^b^a State Key Laboratory of Marine Environmental Science, Xiamen University, Fujian 361005, China^b Fujian Institute of Oceanology, Fujian 361012, China

ARTICLE INFO

Article history:

Accepted 26 January 2011

Available online 25 February 2011

Keywords:

Temperature

Salinity

Upwelling

Variability

Southwestern Taiwan Strait

ABSTRACT

Using the CTD data from four successive summer cruises during 2004–2007, this paper studies the variable temperature, salinity and water mass structures in the southwestern Taiwan Strait in summer. By applying the fuzzy clustering method to the collected CTD data, we classify the hydrographical structure as mainly having five major water masses in the studied area in summer. The variable hydrographical structure is especially demonstrated by the coastal upwelling, which occurred in the sea area near Dongshan with different scales, locations and intensities during the observation period of each cruise. Evident coastal upwelling appeared in the southwestern Taiwan Strait during July of 2005 and 2007. Numerical simulations from a POM-based, high resolution and three-dimensional model explain the observed variable hydrographical structures and show that the variability is largely associated with local wind conditions.

© 2011 Elsevier Ltd. All rights reserved.

1. Introduction

The Taiwan Strait (TWS) is a significant channel connecting the South China Sea (SCS) and the East China Sea, and plays an important role in the water exchange between both seas. It is characterized by rough bottom topography (Fig. 1a) and complicated current systems. Various currents, such as the Zhemina Coastal Current, Yuedong Coastal Current, SCS Warm Current and occasional Kuroshio Intruding Branch, interact with each other within the strait under the influence of monsoon winds (Hu et al., 2010). The growth and decay of these currents induce the variations of temperature, salinity and water mass structures in the TWS, and thus affect the temporal and spatial variations of chemical and biological factors. However, the mechanisms for their variations are quite complex because they are regarded to be affected by variable winds, currents, plumes, tides and bottom topography, as mentioned by Liu et al. (2002) and Xiao et al. (2002) who reviewed the climatological distribution patterns of temperature, salinity and water mass in the TWS and its adjacent areas mostly according to historical observational data.

Since 2002, several intensive studies have been conducted using comprehensive observations, numerical experiments and satellite data (e.g. Jan et al., 2002; Ma et al., 2002; Tang et al.,

2002; Wang et al., 2004; Hong et al., 2005). Tang et al. (2004) examined satellite images (from 1980 to 2002) of two major upwelling zones in the TWS, i.e., Taiwan Bank upwelling and Dongshan upwelling, and revealed the annual variation in both upwelling zones. Jan et al. (2006) analyzed the variability of water masses in the TWS using CTD data (1985–2003) and sectional ADCP data (1999–2001). Wu et al. (2007) constructed a fine-resolution model with realistic bathymetry to study the spatial and temporal variations of the circulation in the TWS. Gan et al. (2009) studied the interaction between the Pearl River plume and the wind-driven coastal upwelling in the TWS. Hong et al. (2009a) applied the empirical orthogonal function analysis to the satellite-derived sea surface temperature data to study the inter-annual variability of coastal upwelling along the Fujian coast of the TWS. Hong et al. (2009b) proposed that the hydrographical structure in the southern TWS was affected by the low salinity water traced back from the Pearl River (the Zhujiang River) in the summer of 2005.

These previous studies have illustrated some basic features of temperature and salinity in the TWS. However, the temperature and salinity structures are quite complex in summer, and several upwelling-related low temperature and high salinity regions have rather large variability. In this paper, Section 2 describes the data sources and data processing method. Section 3 presents the variability based on the in situ data from four successive summer cruises during 2004–2007, referring to the summertime mean hydrographical pattern in the southwestern TWS. Sections 4 and

* Corresponding author.

E-mail address: hujy@xmu.edu.cn (J. Hu).

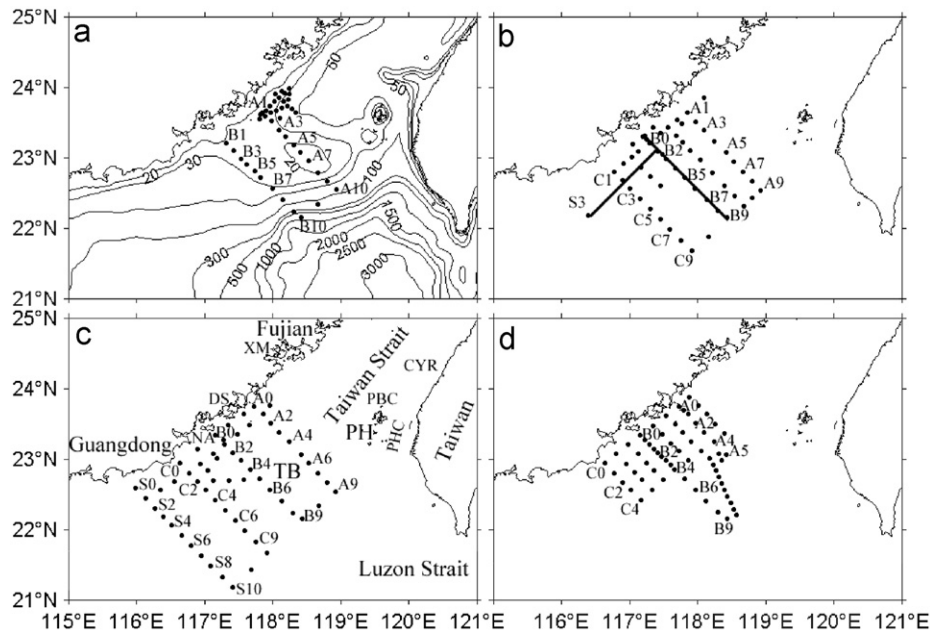


Fig. 1. Sampling stations for four successive summer cruises during 26 July–7 August, 2004 (a), 4–15 July, 2005 (b), 20 June–2 July, 2006 (c) and 8–16 July, 2007 (d). The depth contours are denoted in (a). XM, DS, NA, TB, PH, CYR, PBC and PHC in (c) denotes Xiamen, Dongshan, Nan-ao, Taiwan Bank, Penghu, Changyun Ridge, Pengbei Channel and Penghu Channel, respectively.

5 give a discussion using numerical modeling and a summary of this study, respectively.

2. Data sources and data processing method

The R/V “Yanping 2” was used in four successive summer cruises conducted in the southwestern TWS during July 26–August 7 of 2004, July 4–15 of 2005, June 20–July 2 of 2006 and July 8–16 of 2007. The sampling stations during each cruise are shown in Fig. 1.

During these four cruises, temperature and salinity were measured at each station using an SBE 917plus CTD profiler (Sea Bird Corporation, USA). The specifications of the profiler are as follows: temperature accuracy is 0.001 °C, temperature resolution is 0.0002 °C; conductivity accuracy 0.0003 s m^{-1} and resolution 0.00004 s m^{-1} ; pressure accuracy 0.125 db and resolution 0.0125 db. The CTD sampling interval is 24 Hz.

Based on the obtained CTD data, the temperature and salinity distributions at the surface, 5, 10, 20, 30, 50 m and near-bottom (2–5 m above the sea floor) are mapped. Meanwhile, the vertical and sectional distributions of temperature and salinity are also plotted. Then we classify the water masses using the fuzzy clustering method (Chen and Yao, 1994; Li and Su, 2000).

3. Results

3.1. Average temperature, salinity and water mass distributions in summer

Using the CTD data of four successive summer cruises during 2004–2007, temperature and salinity are averaged if more than three CTD observations have been conducted at the same sampling station. Thus we obtain the summertime mean temperature, salinity and water mass structures for three regular sections in the studied area.

Fig. 2a and b indicate that a low temperature and high salinity zone (the cold core temperature is lower than 24.0 °C) is centered

near Nan-ao in the 5 m layer, while a northeastward low salinity water (with relatively higher temperature) tongue is formed along the coast through the channel west of the Taiwan Bank. The low salinity tongue has a salinity less than 30.0. In addition, in the upper layer over the northeastern Taiwan Bank (near stations A6 and A7), there exists a relatively lower temperature and higher salinity zone, with the temperature lower than 27.0 °C and salinity higher than 33.5.

Below the 10 m layer, the low temperature and high salinity zone becomes a belt along the southern Fujian coast (Fig. 2c–h). In this low temperature and high salinity belt, the cold core appears to the southwest of Nan-ao in the 30 m layer, but moves to the southeast of Nan-ao in the 10 m layer, suggesting that the low temperature and high salinity water comes from the southwest and climbs northeastward from the lower layer to the upper layer. From Fig. 2e–h, it is clearly seen that the temperature and salinity patterns on the western side of the Taiwan Bank are different from those on the eastern side. It has lower temperature and higher salinity down from the 20 m layer on the western side, while it is with relatively higher temperature and higher salinity from 20 m to 30 m depth on the eastern side. This difference is caused by the summertime current patterns (Hu and Liu, 1992), in which a northeastward current flows on the western side whereas an eastward current deflects on the southern side and flows northeastward on the eastern side of the Taiwan Bank. Recently long-term current observations using high frequency radar also exhibited a 10 cm s^{-1} northeastward background current on the western side of the Taiwan Bank (Zhu et al., 2008).

Fig. 3 demonstrates the summertime mean sectional distributions of temperature and salinity for the three studied sections. Low temperature ($T < 24.0$ °C) and high salinity ($S > 34.0$) water appears beneath the 5 m layer at station A1 of Section A (Fig. 3a and b). For the stations between A2 and A6, both temperature and salinity are vertically homogeneous. Another low temperature and high salinity water exists in the lower layer between stations A7 and A10, having a tendency to climb from the lower layer of station A10 to the upper layer of station A7.

Below the 10 m layer of Section B, the stations between B0 and B3 are characterized by low temperature and high salinity water.

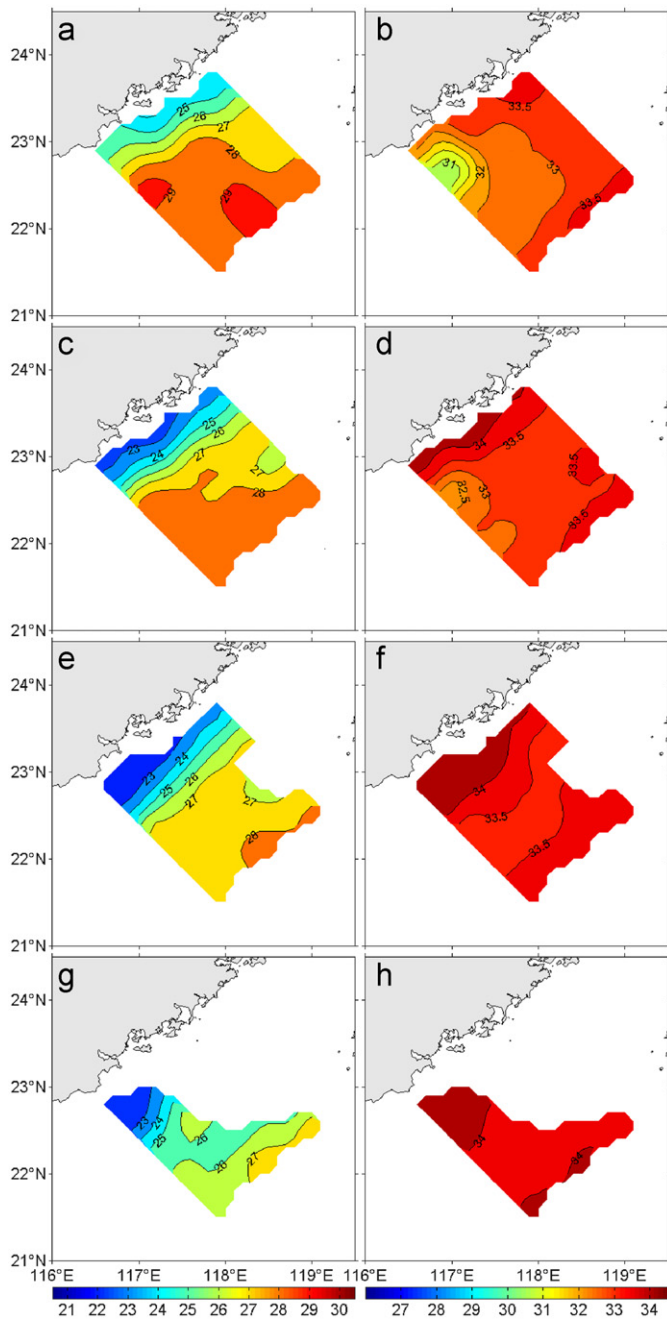


Fig. 2. Summertime mean temperature (a—5 m, c—10 m, e—20 m and g—30 m) and salinity (b—5 m, d—10 m, f—20 m and h—30 m) distribution during 2004–2007.

Between stations B8 and B10, low temperature and high salinity water also exists and it climbs to 20–30 m of station B7 (Fig. 3c and d).

The temperature and salinity patterns in Section C differ from those in the other two sections. Firstly, much lower temperature ($T < 22.0$ °C) water is observed below 20 m at stations between C0 and C2 (Fig. 3e). Secondly, the low temperature and high salinity water climbs towards the upper layer at station C7, but only to 40 m (Fig. 3e and f). Thirdly, low temperature and high salinity waters (i.e., $T < 22.0$ °C and $S > 34.0$) on both sides of the section connect with each other because Section C is not affected by the shoaling Taiwan Bank. On the other hand, a low salinity water exists in the surface layer between stations C0 and C3, with the salinity lower than 30.0 (Fig. 3f).

The water mass classification indicates that five major water masses exist in these three sections (Fig. 4 and Table 1). Coastal Diluted Water exists in the surface layer between stations C0 and C3, with the core salinity of 30.06 and core temperature of 28.58 °C. Subsurface Water appears in the lower layer of some deep water stations in both Section B and Section C, and it is lowest in temperature (15.75 °C) and highest in salinity (34.52), representing the typical SCS water in the subsurface layer (Li, 1987). Upper Warm Water covers the upper layer between stations C4 and C9, stations B2 and B9 and stations A8 and A10, and has the core temperature and salinity of 29.30 °C and 33.01, respectively. Upwelled Water (core temperature: 21.80 °C, core salinity: 34.36) is observed below the surface layer at some near-shore stations and in the 60–120 m layer of some deep water stations (Fig. 4). Mixed Water is sandwiched between the upwelled water and the upper warm water.

3.2. Variability of temperature, salinity and water masses in summer

Fig. 5 presents the time series of the wind vectors for the survey region from the QuikSCAT data. The time series covers the cruise periods in July–August 2004, July 2005, June–July 2006 and July 2007. It is indicated from the panels that the winds were strong but variable in direction during the 2004 cruise (Fig. 5a), and the wind direction was northeasterly before the cruise period since it was affected by a typhoon. During the 2005 cruise, southerly and southwesterly winds dominated before and during the cruise (Fig. 5b) and lasted for about 10 days in the survey area. The southerly wind was weak during the 2006 cruise, while the southwesterly winds prevailed in the survey area and were stable for almost the whole month of July in 2007. Under these different wind conditions, the observational results from the four successive summer cruises indicate that the temperature, salinity and water masses varied in the studied area.

Fig. 6 shows the sectional distributions of temperature during 2004–2007, and demonstrates that the temperature distribution varies from one cruise to another. The most pronounced difference is the low temperature zone (in blue) along the southern Fujian coast. During the cruise in July 2005, the low temperature belt (< 23 °C) covered the area from Nan-ao to Dongshan and appeared beneath the surface layer at some near-shore stations (Fig. 6b). The distribution of the coastal low temperature belt in June–July 2006 (Fig. 6c) was similar to that in July 2005, but had relatively higher temperature. In July 2007, a large scale of low temperature belt covered almost all the near-shore stations of 8 sections in the survey area (Fig. 6d). In contrast, the low temperature belt had the smallest scale (Fig. 6a) in July–August 2004, though this is judged from only three sections conducted in that year.

From the sectional distributions of salinity obtained during 2004–2007 (Fig. 7), it is evident that the salinity also varied from cruise to cruise. In the near-surface layer, low salinity water was clearly seen between stations C1 and C4 during the cruise in July 2005, and between stations C0 and C3 during June–July 2006. The low salinity water even extended to stations B2 and B3 in July 2005 (Fig. 7b) and was traced back from the Pearl River plume (Hong et al., 2009b). As for the cruises both in July–August 2004 and in July 2007, the low salinity water was absent from the survey area.

As shown in Fig. 8, the water mass distribution varied quite a lot for each cruise. Such variations are also reflected by the core temperature and salinity values for each water mass (Table 1).

During the cruise in July–August of 2004, Coastal Diluted Water did not appear in the three surveyed sections, and Upwelled Water only existed near Dongshan on a smaller scale

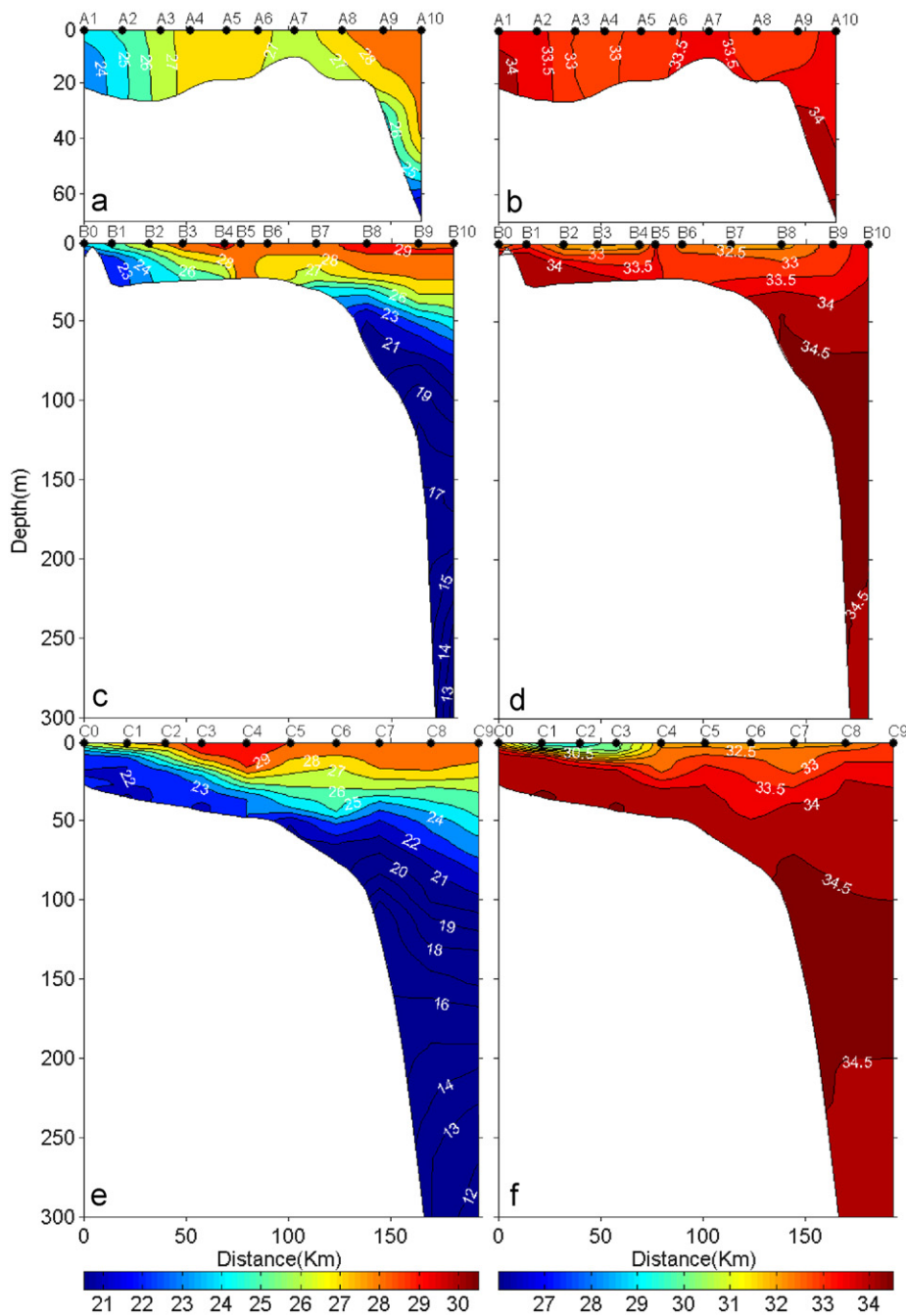


Fig. 3. Summertime mean sectional distributions of temperature (a—Section A, c—Section B and e—Section C) and salinity (b—Section A, d—Section B and f—Section C) during 2004–2007.

(Fig. 8a). Upper Warm Water was dominant in the middle of Section B, characterized by the high temperature of about 29 °C. Subsurface Water located beneath 100–150 m at the deep water stations of Section B with the core temperature of 15.10 °C and core salinity of 34.53. Mixed Water (temperature: 26.09 °C, salinity: 33.95) was between the Upper Warm Water and the Upwelled Water.

There were 5 water masses in the survey area during the cruise in July 2005 (Fig. 8b). Coastal Diluted Water covered the near-surface layer on the near-shore side of the Sections between C and B, with an influence depth of about 10 m and a core salinity of 29.05. Next to the Coastal Diluted Water, Upper Warm Water mainly occupied the upper 25 m layer on the offshore side of

these sections, with a core temperature of 29.46 °C. One Upwelled Water had lower temperature and higher salinity at the near-shore stations of Sections A and B. It even affected the surface layer, with the temperature being 1.20–4.80 °C lower and salinity 0.10–0.85 higher than those in its adjacent areas. Another Upwelled Water existed at the offshore stations of Sections between B and C, having the tendency to climb from 120 to 45 m. The core temperature and salinity of the Upwelled Water was 21.84 °C and 34.40, respectively. The Upwelled Water during the cruise of 2005 had the lowest temperature and highest salinity among the four summertime cruises in 2004–2007. Mixed Water was mostly from 25 to 100 m with a temperature of 24.03 °C and a salinity of 33.91. Subsurface Water, having a

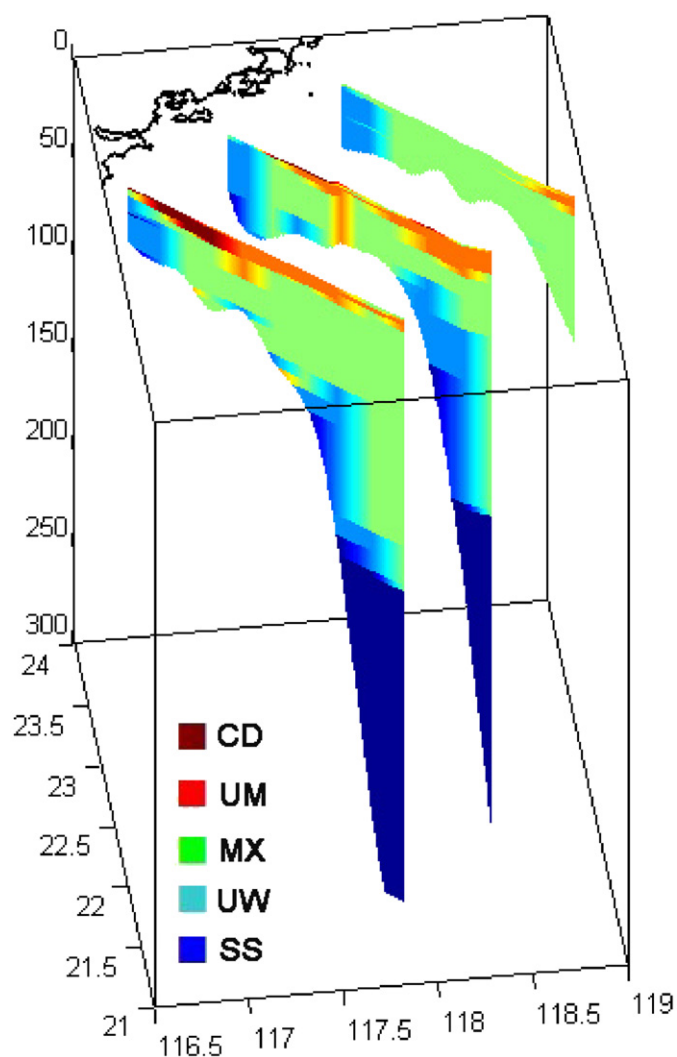


Fig. 4. Summertime mean water mass distribution during 2004–2007. Name of water mass: (1) Coastal Diluted Water (CD in the figure); (2) Upper Warm Water (UM); (3) Mixed Water (MX); (4) Upwelled Water (UW) and (5) Subsurface Water (SS).

Table 1

The core values of temperature and salinity for each water mass.

		Coastal Diluted Water	Upper Warm Water	Mixed Water	Upwelled Water	Subsurface Water
Summertime mean	<i>T</i> (°C)	28.58	29.30	25.49	21.80	15.75
	<i>S</i>	30.06	33.01	33.77	34.36	34.52
Cruise during Jul–Aug 2004	<i>T</i> (°C)		29.37	26.09	22.42	15.10
	<i>S</i>		33.60	33.95	34.31	34.53
Cruise during July 2005	<i>T</i> (°C)	29.05	29.46	24.03	21.84	15.03
	<i>S</i>	30.02	32.73	33.91	34.40	34.54
Cruise during Jun–Jul 2006	<i>T</i> (°C)	28.85	29.14	24.88	21.96	15.37
	<i>S</i>	30.44	32.34	33.83	34.33	34.54
Cruise during July 2007	<i>T</i> (°C)	27.62	29.77	25.30	22.10	17.34
	<i>S</i>	31.65	33.14	33.72	34.38	34.61

temperature of 15.03 °C and a salinity of 34.54, was characterized by low temperature and high salinity and located below the 180 m layer on the offshore side of Sections between C and B.

During the cruise in June–July of 2006, Coastal Diluted Water appeared in the surface layer of some near-shore stations of Sections S, C and B (Fig. 8c). However, it was thinner (only 5 m thick) but wider (extending to stations B7 and C6) than that in the cruise of 2005. Upper Warm Water (core temperature: 29.14 °C) was much smaller in scale, and only distributed in the upper layer (0–25 m) of some central stations in Sections C and S. Upwelled Water was observed in the lower layer of Sections B, C and S. For Sections B and C, the Upwelled Water along the coastal area did not connect with that in the southern Taiwan Bank, because both Upwelled Waters were interrupted by Mixed Water. However, the Upwelled Water climbed from the 180 m layer to the near-surface layer of several near-shore stations at Section S. Down from 180 m depth in the southern Taiwan Bank, Subsurface Water existed with a low temperature of 15.37 °C and a high salinity of 34.54 (Fig. 8c).

Coastal Diluted Water appeared only at station C1 with a core salinity of 31.65 during the cruise in July 2007 (Fig. 8d). Upper Warm Water had a higher temperature of 29.77 °C and existed at the offshore stations of Sections S and B, affecting down to 40 m depth. Upwelled Water covered a large coastal area and affected the near-surface layer. Besides, Upwelled Water could also be seen at 100–170 m depth in the southern Taiwan Bank. Another water mass was Mixed Water whose core temperature and salinity was 25.30 °C and 33.72, respectively. Subsurface Water (temperature: 17.34 °C, salinity: 34.61) lied in the lower layer of several deep water stations in Sections S and B.

Evidently, the hydrographical structure had a large variability in the southwestern TWS during the summers of 2004–2007. The most remarkable variability was indicated by the scale, location and feature of the low temperature and high salinity water or coastal upwelling at some near-shore stations.

4. Discussion

In order to explain the variable temperature and salinity structures, a high resolution, three-dimensional, hydrodynamic model has been developed. This model is based on the Princeton Ocean Model (POM; Mellor, 2004), and a nested strategy is introduced in the modeling system. Horizontally, the whole domain covers the Northwest Pacific with a 1/5° coarse grid, and the sub-domain is zoomed in to the TWS and its adjacent area (116.5–125.5°E, 18.1–27.7°N) with a 1/25° fine grid. There are 21 sigma levels in the vertical. The daily fluxes at the air–sea interface are downloaded from the National Center for Environmental Prediction (Kalnay et al., 1996). The monthly climatological thermohaline parameters along the open boundaries come from a Pacific Regional Ocean Model System (Liu and Chai, 2009), and the monthly mean runoff is set for each river along the China coast. The details about the construction and verification of the model were given by Jiang (2007) and Jiang et al. (submitted for publication). Tide is not considered for the present study. After spin-up and verification, the model is run continuously from the beginning of 1999 to the end of 2007. This paper uses some of the model simulation results to discuss the observed variability of hydrographical structure.

As shown in Fig. 5b, the upwelling-favoring winds lasted for about 10 days during the summer cruise of 2005, so the strong coastal upwelling, characterized by the low temperature and high salinity water, had been induced in the southwestern TWS (Figs. 6 and 7). According to the verified numerical modeling results, the 2005 cruise is herewith set as an example to illustrate the relationship between the hydrographical structure and the local wind conditions, circulation and bottom topography.

Fig. 9 presents the calculated temperature and current distributions at 10, 20, 30 and 40 m depths during the CTD mapping

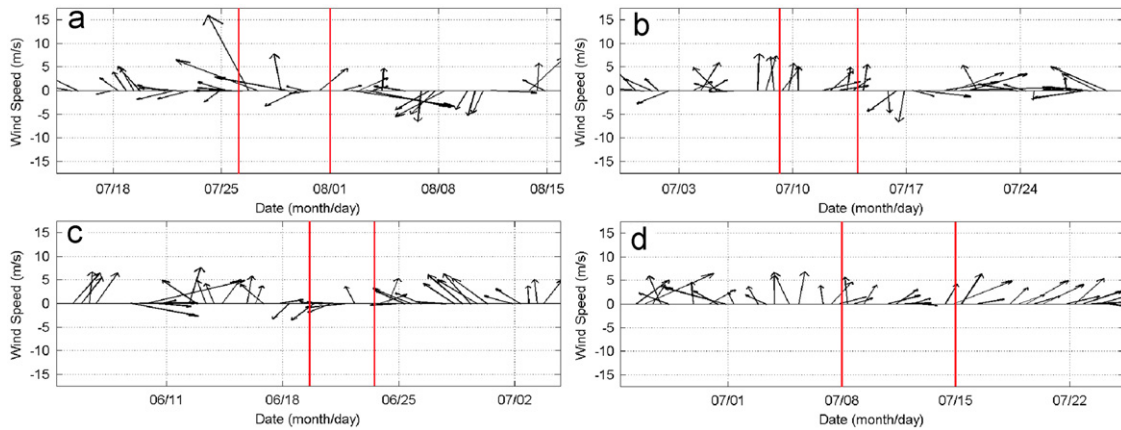


Fig. 5. Daily wind vector at the survey region for the period covering each cruise. The cruise observation of CTD mapping period is denoted by two red lines. (a) Cruise in July–August, 2004; (b) cruise in July, 2005; (c) cruise in June–July, 2006 and (d) cruise in July, 2007. (For interpretation of the references to color in this figure legend, the reader is referred to the web version of this article.)

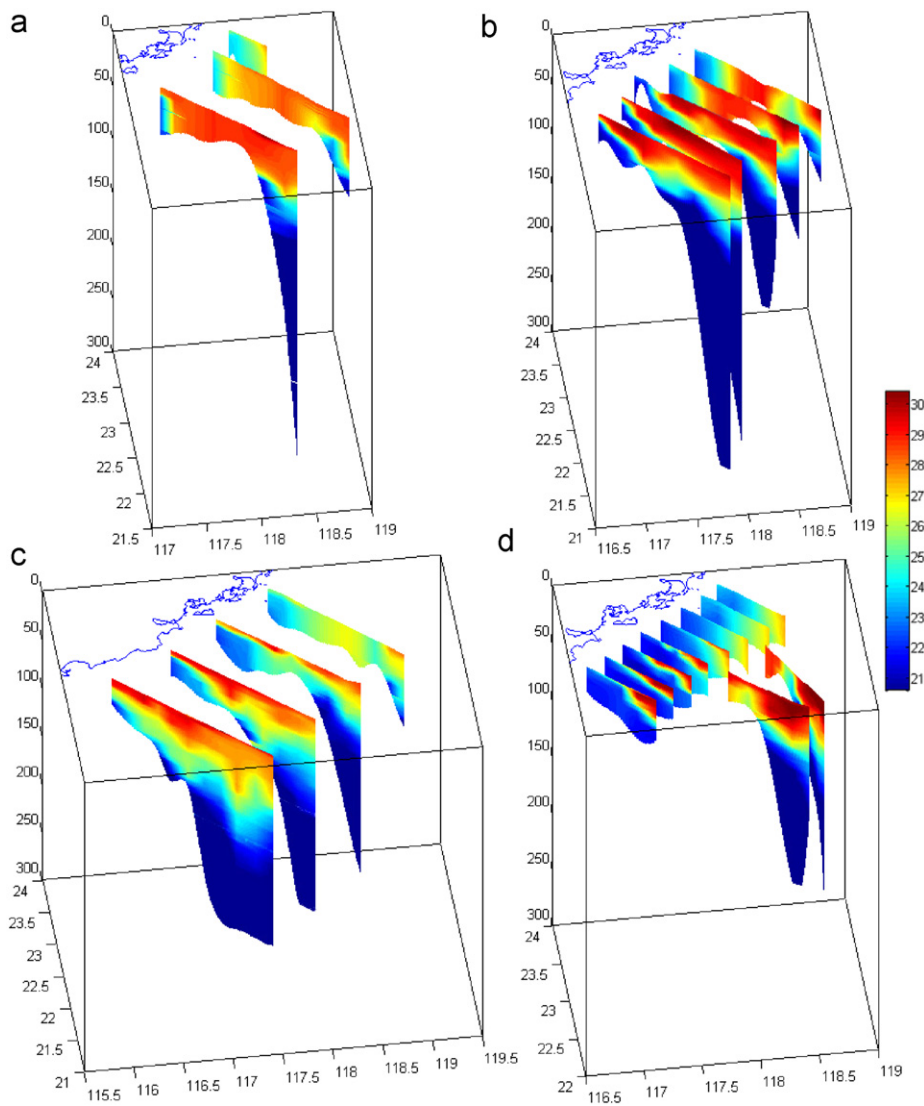


Fig. 6. Sectional temperature distribution for summer cruises during 2004–2007. (a) Cruise in July–August, 2004; (b) cruise in July, 2005; (c) cruise in June–July, 2006; and (d) cruise in July, 2007. (For interpretation of the references to color in this figure, the reader is referred to the web version of this article.)

period of July 9–14, 2005. At 10 m, a low temperature water ($T < 23$ °C; also with relatively higher salinity, but the salinity distribution is omitted here to avoid the verbosity) existed in the

southwestern TWS. Besides, two relatively lower temperature zones appeared around the Taiwan Bank. As for the current distribution, there existed a northeastward flowing current in

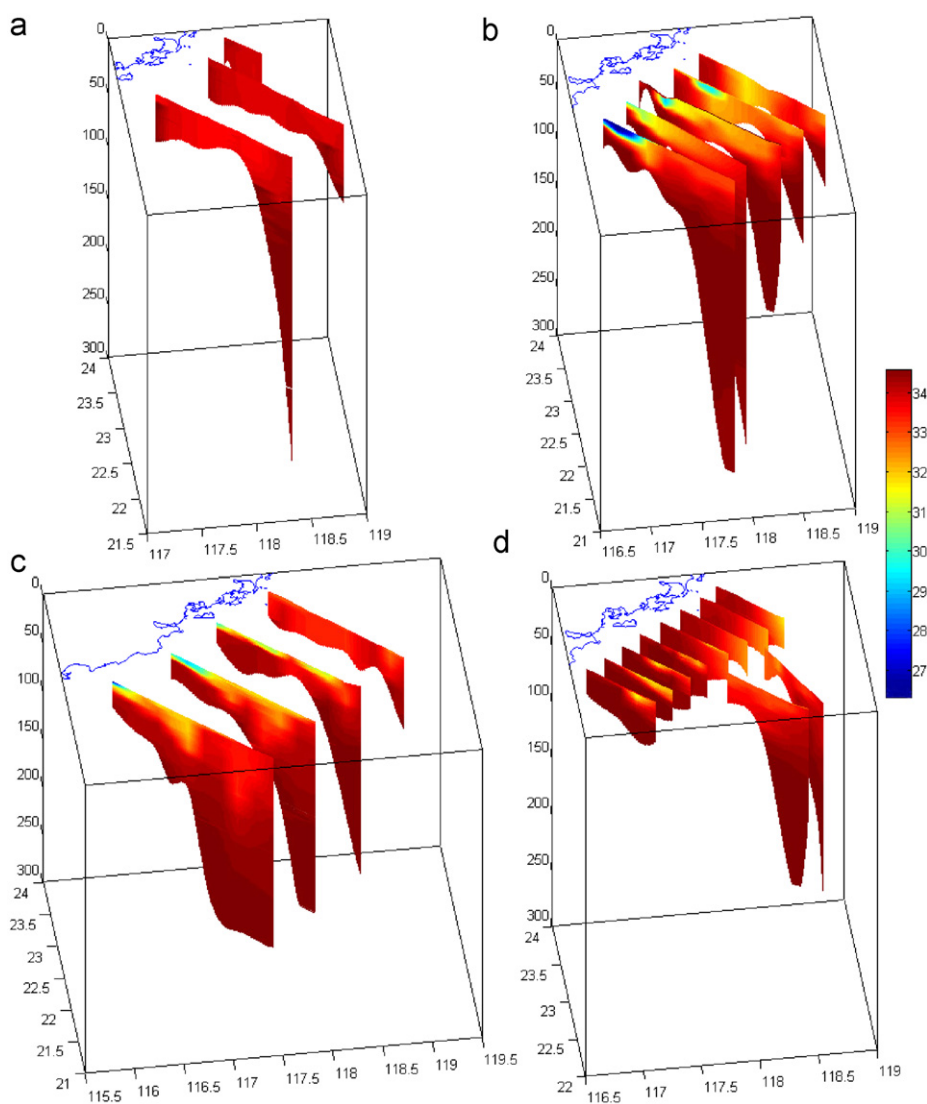


Fig. 7. Sectional salinity distribution for summer cruises during 2004–2007. (a) Cruise in July–August, 2004; (b) cruise in July, 2005; (c) cruise in June–July, 2006 and (d) cruise in July, 2007.

the channel west of the Taiwan Bank, which flowed along the coast near Nan-ao and Dongshan. Another current, bringing with relatively higher temperature water, flowed eastward in the southern Taiwan Bank and turned northward through the Penghu Channel southwest of Taiwan. The calculated circulation pattern in the southern TWS agreed well with the summertime climatology summarized by Hu and Liu (1992). At 20 m, the low temperature water formed a long belt along the Fujian coast. The coldest zone appeared near the south and southwest of Nan-ao (Fig. 9b). The current pattern was almost the same as that at 10 m. As for the 30 and 40 m layers, the western TWS was still characterized by low temperature, especially along the southern Fujian coast and around the Taiwan Bank, while the eastern TWS was dominated with relatively higher temperature water (Fig. 9c and d).

Using the numerical model simulation, Fig. 10 demonstrates two 3D pictures of sectional temperature distribution with along-section current vectors for Sections B0–B9 and S3–B2 (the section locations are shown in Fig. 1b). The simulated pattern (Fig. 10a) matched quite well with the observed one (Fig. 6b) during the same period. The southerly and southwesterly winds prevailed in the southern TWS on July 10 of 2005 (Fig. 5b), the temperature distribution in Section B0–B9 (Fig. 10a) showed clearly cold water

beneath the surface layer near Nan-ao. Fig. 10a also indicates that a northward current brought the cold water from the subsurface layer of station S3 and then climbed towards the near-surface layer of stations B0 and B2 so as to generate the upwelling-related low temperature zone there. As for Section B0–B9, the along-section current was mostly offshore, which transported the upper layer water from the coast and from the Taiwan Bank, inducing the cold water to upwell near stations between B0 and B2 and near the Taiwan Bank (i.e. stations B6 and B7). In contrast, the distributions of temperature and along-section current (Fig. 10b) were quite different under the northeasterly winds. The thermocline layer was not lifted to the near-surface layer and the along-section current weakened. Evidently, different wind conditions generated different circulations to cause the variability of hydrographical structure in the southwestern TWS.

In summer, the thermocline is usually observed between 10 and 30 m layer in the southern TWS (Hu and Fu, 1998). Following Su and Pohlmann (2009), the isotherms in the 30 m layer are considered as the indicator of the thermocline lifting associated with the upwelling. Fig. 11 illustrates the variations of temperature and current at 30 m depth in July 2005. The typical temperature distribution pattern was the relatively lower temperature water in the western TWS and around the Taiwan Bank,

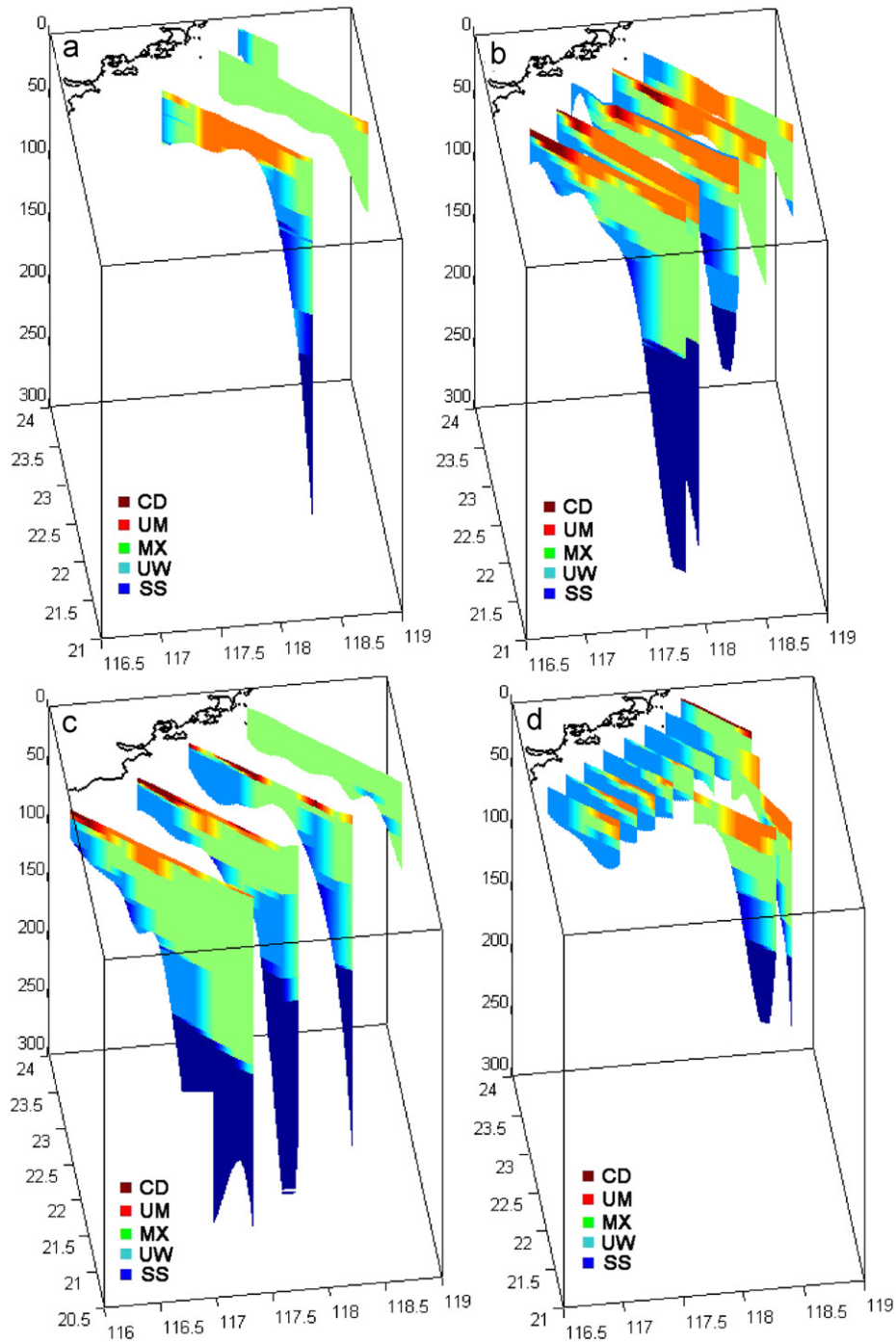


Fig. 8. Sectional water mass distribution for summer cruises during 2004–2007. (a) Cruise in July–August, 2004; (b) cruise in July, 2005; (c) cruise in June–July, 2006 and (d) cruise in July, 2007. Name of water mass: (1) Coastal Diluted Water (CD in the figure); (2) Upper Warm Water (UM); (3) Mixed Water (MX); (4) Upwelled Water (UW) and (5) Subsurface Water (SS).

but its scale varied from time to time. In the first half of July 2005, the southwesterly and southerly winds prevailed in the southwestern TWS (Fig. 5b). The strong coastal upwelling was thus induced. The broad range of the cold water was observed in the 30 m layer along the Fujian coast (Fig. 11a–c, temperature distributions on July 5, 10 and 15). In the latter half of July, the wind direction was variable from northerly to southeasterly (Fig. 5b). Such unstable wind was not favorable for coastal upwelling so that the cold water appeared in a much smaller scale in the western TWS during this period (Fig. 11d–f).

As for the influence of topography on the upwelling, many related researches have been conducted. MacCready and Rhines (1993) explored the slippery bottom boundary layers on a slope through theory and numerical simulation. Oke and Middleton (2000) studied the topographically induced upwelling off the eastern Australia. Song and Chao (2004) conducted a theoretical study of topographic effects on coastal upwelling and cross-shore exchange. Su and Pohlmann (2009) applied a numerical model to study the coastal upwelling off the eastern Hainan Island and examined the wind, topography and bottom boundary layer's

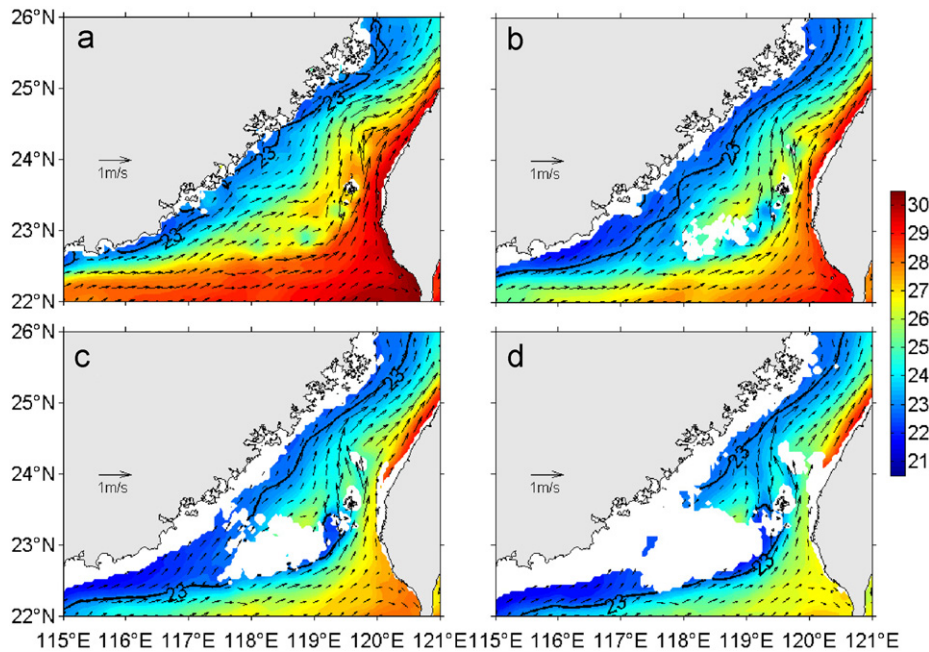


Fig. 9. Distribution of temperature and current during the cruise CTD mapping period of July 9–14, 2005. (a) 10 m layer, (b) 20 m layer, (c) 30 m layer and (d) 40 m layer. 23 °C isotherm is denoted.

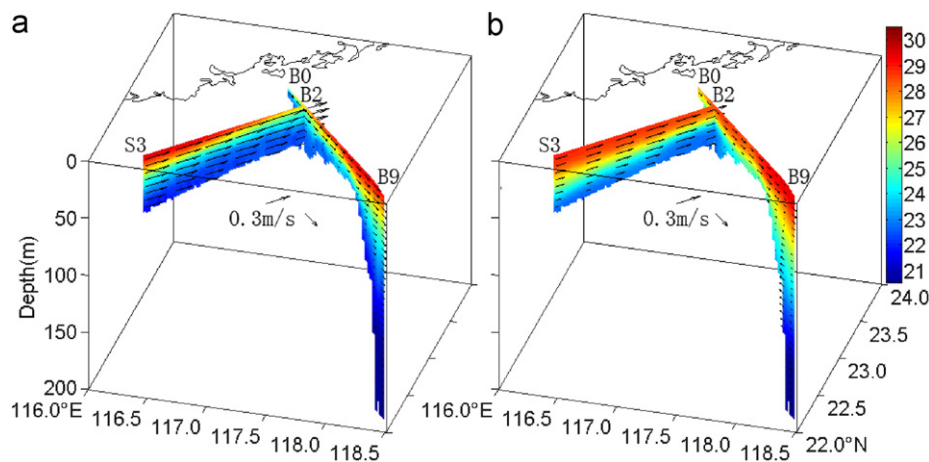


Fig. 10. Distribution of temperature and along-section current in Section B0–B9 and Section S3–B2. (a) During southwesterly winds and (b) during northeasterly winds. Section locations are shown in Fig. 1(b).

influences on the upwelling. By setting several transects pointing to the upwelling center in different directions, Jiang et al. (submitted for publication) analyzed the topographic influence on the upwelling and proposed that the topography plays an important role in inducing three main upwelling regions in the TWS, and that the upwelled water near-shore of Dongshan is driven from the subsurface layer of the SCS via the deep channel west of the Taiwan Bank. From these researches, it is suggested that the topography and bottom boundary layer should also be considered when studying the variability of upwelling or hydrographical structure in the TWS. A diagnostic analysis on the numerical model results is required for this purpose in future.

It is clear from the above simulation results that the temperature, salinity and water mass structures vary markedly associated with local wind conditions. The southwesterly or southerly wind is favorable for inducing coastal upwelling, while the northerly or variable wind is unfavorable for observing coastal upwelling events there. Coastal upwelling usually responds very quickly to wind with a lag time of only one or two days.

5. Conclusions

Using the CTD data obtained in four successive summer cruises during 2004–2007 and the numerical model simulation results covering the periods of observation, variable temperature, salinity and water mass structures are characterized in the southwestern TWS in summer.

Based on the collected CTD data, the summertime mean water mass structure has been classified using the fuzzy clustering method. It is indicated that the studied area is dominated by Mixed Water (temperature: 25.49 °C, salinity: 33.77), accompanied by several other water masses. One is Upper Warm Water mostly covering the upper layer of the southern TWS. Another is Upwelled Water (with a temperature of 21.80 °C and a salinity of 34.36) located in the lower layer east of Nan-ao and in the 30–130 m layer southeast of the Taiwan Bank. The third is the low salinity Coastal Diluted Water (temperature: 28.58 °C, salinity: 30.06) distributed in the surface layer of the western Taiwan Bank. For the area southeast of the Taiwan Bank, the low

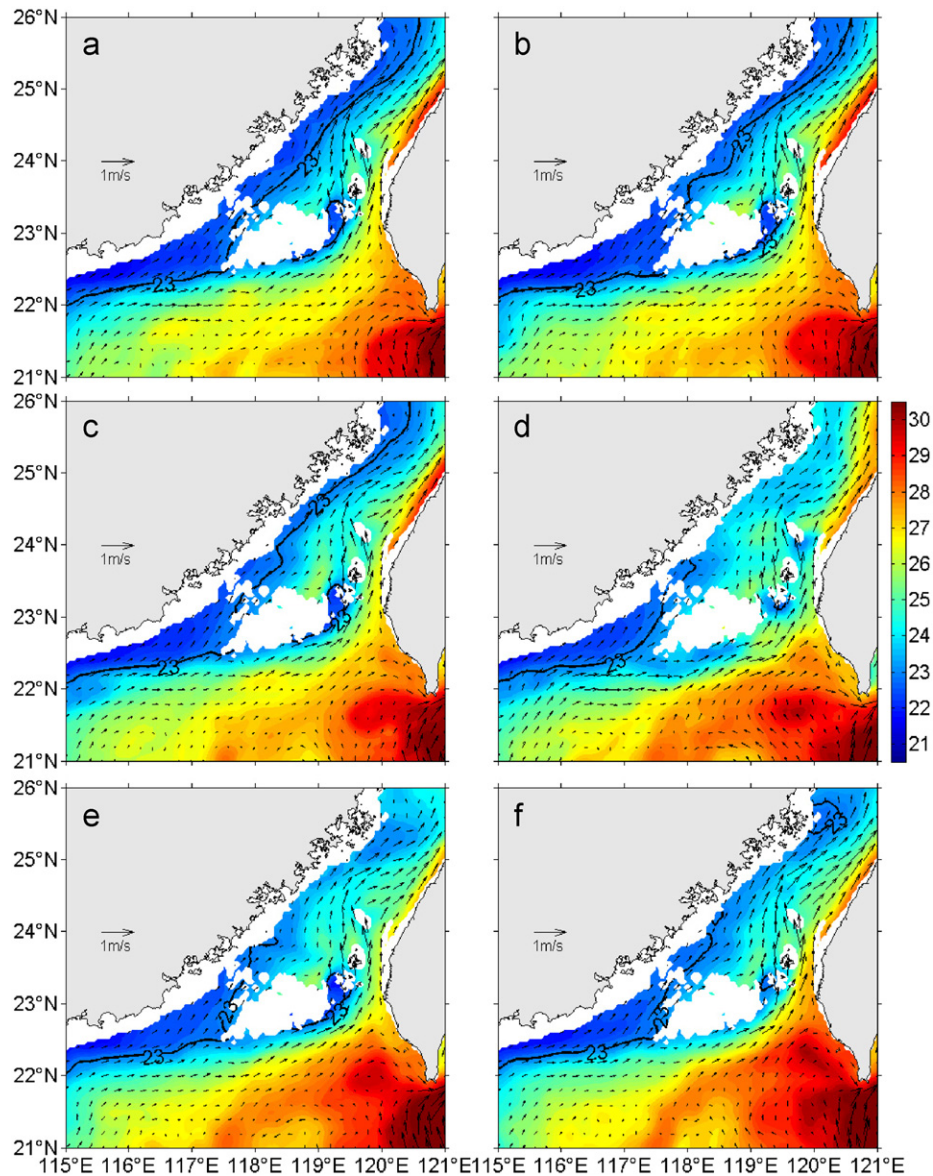


Fig. 11. Daily mean temperature and current distribution in the 30 m layer in July 2005. (a) July 5, (b) July 10, (c) July 15, (d) July 20, (e) July 25 and (f) July 30. 23 °C isotherm is denoted.

temperature and high salinity Subsurface Water exists below the 130 m layer.

The variability in hydrographical structure, being further investigated from the specific cruise data, is also represented by the scale of coastal upwelling. The coastal upwelling in the area near Dongshan had different scales, locations and intensities during the four cruises. During the cruise in July–August of 2004, it located to the northeast of Dongshan. The size of the upwelling zone was small, and the upwelling did not have the evident low temperature or high salinity feature in the surface layer. During the cruise in July 2005, a broader scale low temperature and high salinity water appeared near the surface layer along the coasts of Eastern Guangdong and Southern Fujian, and two low temperature and high salinity centers occurred to the east of Dongshan and southeast of Nan-ao with the temperature lower than 23.0 °C and salinity higher than 34.0. During the cruise in June–July of 2006, the coastal upwelling mainly existed to the south of Nan-ao. During the cruise in July 2007, a much broader scale of low temperature and high salinity

water appeared near the surface layer along the southern Fujian coast.

Numerical model simulation results from a POM-based, high resolution and three-dimensional model explain the variable hydrographical structures observed during the four summer cruises and show that these variations were largely associated with local wind conditions. When the strong and stable south-westerly winds prevail in the TWS for a few days, evident coastal upwelling can be induced near Nan-ao and Dongshan. The coastal upwelling water appears to come from the subsurface layer of the northern SCS, and the channel west of the Taiwan Bank becomes a pathway for the nutrient-rich water from the subsurface layer of the northern SCS to enter the near-surface layer near Nan-ao and Dongshan.

In addition, the bottom topography, coastal line, local circulation, eddies and tides may also affect the hydrographical structure and induce short-term variations of temperature and salinity. Such short-term variations were demonstrated by repeated observations and numerical modeling, and the variations clearly

respond to variable wind conditions. This deserves further studies in the near future.

Acknowledgements

This study was jointly supported by the NSFC under contracts 40331004, 40810069004 and 40821063; and by the National Basic Research Program of China (2009CB421208). The authors thank the crew of the R/V “Yanping 2” for help during field work. Professors John Hodgkiss and Huijie Xue are acknowledged for their help with English and Mr. Z.D. Huang for his help with figures. Valuable comments and suggestions from two anonymous reviewers and guest editor are also greatly appreciated.

References

- Chen, S.J., Yao, S.Y., 1994. Division of hydroclimatic area over China Seas – II. Cluster analysis and fuzzy ISODATA. *Acta Oceanologica Sinica* 13 (2), 213–224.
- Gan, J.P., Li, L., Wang, D.X., Guo, X.G., 2009. Interaction of a river plume with coastal upwelling in the northeastern South China Sea. *Continental Shelf Research* 29, 728–740.
- Hong, H.S., Shang, S.L., Zhang, C.Y., Huang, B.Q., Hu, J.Y., Huang, J.Q., Lu, Z.B., 2005. Evidence of ecosystem response to the interannual environmental variability in the Taiwan Strait. *Acta Oceanographica Sinica* 27 (2), 63–69 (in Chinese with English abstract).
- Hong, H.S., Zhang, C.Y., Shang, S.L., Huang, B.Q., Li, Y.H., Li, X.D., Zhang, S.M., 2009a. Interannual variability of summer coastal upwelling in the Taiwan Strait. *Continental Shelf Research* 29, 479–484.
- Hong, H.S., Zheng, Q.A., Hu, J.Y., Chen, Z.Z., Li, C.Y., Jiang, Y.W., Wan, Z.W., 2009b. Three-dimensional structure of a low salinity tongue in the southern Taiwan Strait observed in the summer of 2005. *Acta Oceanologica Sinica* 28 (4), 1–7.
- Hu, J.Y., Fu, Z.L., 1998. Regional characteristics of vertical distributions of temperature and salinity in southwestern Taiwan Strait in June, 1988. *Tropic Oceanology* 17 (2), 15–23 (in Chinese with English abstract).
- Hu, J.Y., Kawamura, H., Li, C.Y., Hong, H.S., Jiang, Y.W., 2010. Review on current and seawater volume transport through the Taiwan Strait. *Journal of Oceanography* 66 (5), 591–610.
- Hu, J.Y., Liu, M.S., 1992. The current structure during summer in southern Taiwan Strait. *Tropic Oceanology* 11 (4), 42–47 (in Chinese with English abstract).
- Jan, S., Sheu, D.D., Kuo, H.M., 2006. Water mass and throughflow transport variability in the Taiwan Strait. *Journal of Geophysical Research* 111 (C12), C12012.
- Jan, S., Wang, J., Chern, C.S., Chao, S.Y., 2002. Seasonal variation of the circulation in the Taiwan Strait. *Journal of Marine Systems* 35 (3–4), 249–268.
- Jiang, Y.W., 2007. The now-cast system for the current of the Taiwan Strait, a study of three-dimensional numerical model. Technical Report, State Key Laboratory of Marine Environmental Science, Xiamen University, Xiamen, Fujian, China.
- Jiang, Y.W., Chai, F., Wan, Z.W., Hu, J.Y., Hong, H.S., Characteristics, water sources and mechanisms of the upwelling in the Taiwan Strait: a three-dimensional numerical model study. *Journal of Oceanography*, submitted for publication.
- Kalnay, E., Kanamitsu, M., Kistler, R., Collins, W., Deaven, D., Gandin, L., Iredell, M., Saha, S., White, G., Woollen, J., Zhu, Y., Leetmma, A., Reynolds, B., Chelliah, M., Ebisuzaki, W., Higgins, W., Janowiak, J., Mo, K.C., Ropelewski, C., Wang, J., Jenne, R., Joseph, D., 1996. The NCEP/NCAR 40-year reanalysis project. *Bulletin of the American Meteorological Society* 77, 437–471.
- Li, F.Q., Su, Y.S., 2000. Analyses of Water Masses in Oceans. Qingdao Ocean University Press, Qingdao 397 pp (in Chinese).
- Li, L., 1987. Scatter diagrams of South China Sea T–S character and their brief description. *Journal of Oceanography in Taiwan Strait* 5 (1), 93–95 (in Chinese with English abstract).
- Liu, G., Chai, F., 2009. Seasonal and interannual variability of primary and export production in the South China Sea: a three-dimensional physical-biogeochemical modeling study. *Journal of Marine Sciences* 62 (2), 420–431.
- Liu, J.F., Liu, Z., Ren, S., Zhang, G.Y., 2002. Analysis of hydrographic elements features in Taiwan Strait. *Marine Forecasts* 19 (3), 22–32 (in Chinese with English abstract).
- Ma, Z.J., Wang, C.Y., Xu, J., Nie, F.J., Zhang, J., 2002. Study on the transverse structures across Taiwan Strait. *Science in China series D (Earth Sciences)* 45 (12), 1114–1126 (in Chinese with English abstract).
- MacCready, P., Rhines, P.B., 1993. Slippery bottom boundary layers on a slope. *Journal of Physical Oceanography* 23 (1), 5–22.
- Mellor, G.L., 2004. Users guide for a three-dimensional, primitive equation, numerical ocean model, Program in Atmospheric and Oceanic Sciences, Princeton University, 53pp.
- Oke, P.R., Middleton, J.H., 2000. Topographically induced upwelling off eastern Australia. *Journal of Physical Oceanography* 30 (3), 512–531.
- Song, Y.T., Chao, Y., 2004. A theoretical study of topographic effects on coastal upwelling and cross-shore exchange. *Ocean Modelling* 6 (2), 151–176.
- Su, J., Pohlmann, T., 2009. Wind and topography influence on an upwelling system at the eastern Hainan coast. *Journal of Geophysical Research* 114, C06017.
- Tang, D.L., Kawamura, H., Guan, L., 2004. Long-time observation of annual variation of Taiwan Strait upwelling in summer season. *Advances in Space Research* 33 (3), 307–312.
- Tang, D.L., Kester, D.R., Ni, I.H., Kawamura, H., Hong, H.S., 2002. Upwelling in the Taiwan Strait during the summer monsoon detected by satellite and shipboard measurements. *Remote Sensing of Environment* 83 (3), 457–471.
- Wang, Y.H., Chiao, L.Y., Lwiza, K.M.M., Wang, D.P., 2004. Analysis of flow at the gate of Taiwan Strait. *Journal of Geophysical Research* 109 (C2), C02025.
- Wu, C.R., Chao, S.Y., Hsu, C., 2007. Transient, seasonal and interannual variability of the Taiwan Strait current. *Journal of Oceanography* 63 (5), 821–833.
- Xiao, H., Guo, X.G., Wu, R.S., 2002. Summarization of studies on hydrographic characteristics in Taiwan Strait. *Journal of Oceanography in Taiwan Strait* 21 (1), 126–138 (in Chinese with English abstract).
- Zhu, D.Y., Li, L., Li, Y., Guo, X.G., 2008. Seasonal variation of surface currents in the southwestern Taiwan Strait observed with HF radar. *Chinese Science Bulletin* 53 (15), 2385–2391.